Enhanced electrochromic performance of composite films by combination of polyoxometalate with poly(3,4-ethylenedioxythiophene)†

Shuping Liu, Lin Xu,* Fengyan Li, Bingbing Xu and Zhixia Sun

Received 26th July 2010, Accepted 19th October 2010
DOI: 10.1039/c0jm02412k

A composite film containing poly(3,4-ethylenedioxythiophene) (PEDOT), polyoxometalate (POM) clusters $K_6P_2W_{18}O_{62}\cdot 14H_2O$ (P_2W_{18}) and polyallylamine hydrochloride (PAH) was fabricated by a smart combination of layer-by-layer (LbL) with electro-polymerization methods. The composite film displays enhanced electrochromic performance by incorporation of P_2W_{18} into the PEDOT film. The electrochromic property of the film is significantly improved, resulting in an optical contrast of 54.7% at 600 nm and an absorbance that does not change after 1500 cycles. Additionally, the film provides broader absorption throughout the visible region. These results demonstrate the essential role of POMs in improving functionality on PEDOT for applications in electrochromic devices.

1 Introduction

Composite materials have received much attention in both chemistry and materials science in recent years, mainly relating to their potential applications in sensors, fuel-cells and light-emitting diodes.[1] Current research in composite materials has focused on the development of organic–inorganic composite materials which endues both opportunity and challenge. The main opportunity is to combine different components with distinct properties in a single system; which will synergistically improve performance or produce multifunctional properties. Meanwhile, it still remains a great challenge to design organic–inorganic composite materials with high stability, switchability, multifunctionality, as well as the facility of tailoring and processing.

In recent years, conductive polymers have been extensively studied as an active material in rechargeable batteries, electrochemical supercapacitors, photovoltaics, and electrochromic devices.[2] Among these conducting polymers, poly(3,4-ethylenedioxythiophene) (PEDOT) has aroused much interest as the blue component for the realization of RGB-based display devices. PEDOT with its low band gap, good environmental stability and high material compatibility has proven to be an excellent candidate for electrochromic materials.[3] However, PEDOT-based films still show drawbacks in terms of their practical application for electrochromic devices. For example, low optical contrast ($\Delta T\%$) and poor stability remain as disadvantages in the fabrication of real devices.[4,5]

Polyoxometalates (POMs), a well-known class of transition metal oxide nanoclusters with intriguing structures and diverse properties,[6] have been combined with conducting polymers in films to enhance their properties. Gómez-Romero and co-workers presented three electrodes made of molecular nanocomposite materials $PAni/H_4SiW_{12}O_{40}$, $PAni/H_3PW_{12}O_{40}$ and $PAni/H_3PMo_{12}O_{40}$ (PAni: polyaniline), which displayed promising specific capacitance values and good cycling stability.[7] Recently, electrically conducting a PEDOT film doped with silicomolybdate ($SiMo_{12}$) has been prepared by electrochemical polymerization.[8] The synthesized film exhibited fast charge propagation and electrocatalytic activity for the reduction of bromate and the oxidation of ascorbic acid. Although POMs should be a promising active component to tune the electrochromic properties of PEDOT, the effect of POMs on the electrochromic performance of PEDOT-based films has been virtually unexplored so far. Furthermore, an arduous task is to find a reasonable method to fabricate an electrochromic film based on POMs and PEDOT.

In this paper, we present a composite film containing $K_6[P_2W_{18}O_{62}]\cdot 14H_2O$ (P_2W_{18}), polyallylamine hydrochloride (PAH), and PEDOT by the smart combination of layer-by-layer self-assembly (LbL) with electro-polymerization methods. The multilayer film is synthesized by forming a P_2W_{18} layer with PAH using the LbL technique, followed by deposition of a PEDOT layer using electro-polymerization in aqueous solution. From the experimental results, the composite film displays enhanced electrochromic performance by combination of PEDOT with P_2W_{18}. The optical contrast and electrochemical cycling stability of the composite film are found to be higher than those of the PEDOT-only film.

2 Experimental

2.1 Materials

P_2W_{18} was prepared according to the literature method.[9] 3,4-Ethylenedioxythiophene (EDOT, Aladdin China) was used as received. 3-Aminopropyltrimethoxysilane (APS), poly(styrenesulfonate) (PSS) (MW 70000) and PAH (MW 70000) were purchased from Aldrich and were used without further treatment. Other reagents were of AR grade. The water used in all experiments was deionized to a resistivity of 18 MΩ cm.

Key Laboratory of Polyoxometalates Science of Ministry of Education, College of Chemistry, Northeast Normal University, Changchun, 130024, P.R. China. E-mail: linxu@nenu.edu.cn; Fax: +86 431 8509 9668; Tel: +86 431 8509 9668

† Electronic Supplementary Information (ESI) available: CV of the $[P_2W_{18}–PAH]_{10}$ and $[PEDOT]_{10}$ films and the relationship between peak potentials of last redox peaks of the $[P_2W_{18}–PEDOT]_{20}$ and pH. See DOI: 10.1039/c0jm02412k/

2.2 Preparation of films

The substrate (ITO glass) was dipped into the APS solution for 8 h, then immersed in HCl (pH = 2.0) for 20 min to form the precursor film. Then the precursor film was alternately dipped into P_2W_{18} (5×10^{-3} M, pH = 4.0 NaAc–HAc buffer solution), PAH (5×10^{-3} M containing 1 M NaCl; pH = 4.0) and P_2W_{18} solution for 8 min, and then electropolymerized in the Na_2SO_4–H_2SO_4 buffer solution (pH = 3.0) containing 0.01 M EDOT and 0.1 M $LiClO_4$ with Ag/AgCl (3 M KCl) as the reference electrode and a platinum coil as the counter electrode. The film was electrodeposited in the potential range of 0.3 to 0.9 V with a sweep rate of 100 mV s^{-1} for a half cycle. After the deposition of each layer, the substrate was rinsed with deionized water and dried in nitrogen. This sequence can be repeated until the desired number of [P_2W_{18}/PAH/P_2W_{18}/PEDOT] (referred to as [P_2W_{18}–PEDOT]) layers is obtained. The [P_2W_{18}–PAH]$_n$ film was prepared on ITO by depositing P_2W_{18} and PAH for 8 min, respectively. The [PEDOT]$_{10}$ film was fabricated by first dipping PSS (5×10^{-3} M containing 1 M NaCl; pH = 4.0) for 8 min, and then electrosynthesized by sweeping the potential from 0.3 to 0.9 V with the scan rate of 100 mV s^{-1} for 10 cycles. All the fabrication processes were performed at room temperature.

2.3 Characterization

All the electrochemical experiments were performed on a CHI 605C electrochemical workstation (Shanghai Chenhua Instrument Factory, China). A conventional three electrodes system was used, with the ITO electrode coated by the self-assembled film as the working electrode, Ag/AgCl (3 M KCl) as the reference electrode and platinum coil as the counter electrode. Spectroeletrochemical measurements of the films were performed by combining the *in situ* Varian Cary 50 Conc UV-vis spectrophotometer with the electrochemical workstation. The electrolyte was 0.1 M $LiClO_4$ in Na_2SO_4–H_2SO_4 buffer solution (pH = 3). Scanning electron micrographs (SEM) were obtained with a Hitachi S-4800 instrument. Atomic force microscopy (AFM) images were taken on a ITO glass using a SPVA 400 instrument.

3 Results and discussion

3.1 Film fabrication

On the one hand, the LbL method which relies on alternate electrostatic absorption of oppositely charged species has been widely utilized to construct POMs-based films. On the other hand, electro-polymerization is a commonly used technique for the preparation of PEDOT films. Electro-polymerization has been used to fabricate films based on POMs and PEDOT, but it is difficult to efficiently control the relative concentration of POMs and PEDOT. To solve this problem, we demonstrated the facile fabrication of a composite film based on P_2W_{18} and PEDOT by a unique combination of LbL and electro-polymerization methods. The formation of two kinds of layers primarily relies on coulombic interactions between the negative charged P_2W_{18} and the positive charged centers on the polymer backbone of PEDOT. Fig. 1 illustrates the schematics of the fabrication of a [P_2W_{18}–PEDOT]$_{20}$ film.

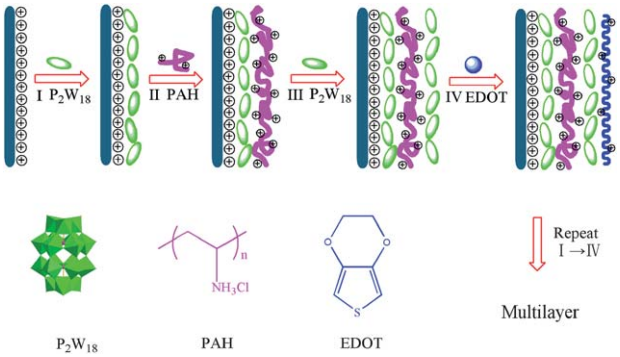

Fig. 1 Schematics of the formation of a [P_2W_{18}–PEDOT] film.

For the [P_2W_{18}–PEDOT]$_{20}$ film, the anionic P_2W_{18} was assembled with cationic PAH in pH = 4 buffer solution as has been demonstrated previously.[10] To increase the surface coverage of the electroactive species, two methods were used to increase film thickness. First, 1M NaCl was added to the PAH solution to reduce the electrostatic repulsion of PAH chains. PAH coils become denser and denser so that the rather small P_2W_{18} anions adsorb at the top of the PAH surface and also disperse into the PAH matrix, which results in an increase of adsorbed P_2W_{18} anions. Second, a higher P_2W_{18} concentration was used here because the film was easily accessed by P_2W_{18} particles.[11] In other words, high component concentration generally improves the adsorption kinetics. PEDOT films are generally formed from organic media or aqueous solutions with surfactants. However, in this article the PEDOT film was prepared in an aqueous medium involving a traditional lithium ion conducting liquid. During the polymerization process, the electrode potential and monomer concentration are the most critical parameters to control. The potential value (+0.9 V) was selected as it meant that the polymer was not over-oxidized so as to avoid the decrease in the conductivity or even the destruction of the film.[12] A low monomer concentration (0.01 M) was chosen because the polymerization proceeds easily.[13] Additionally, two means were employed to form uniform and long-term stable films. The EDOT monomer was dispersed in an aqueous acidic medium *via* ultrasonication for about 10 min. The aqueous solvent (pH = 3 Na_2SO_4–H_2SO_4 buffer solution) served as the electrolyte. To optimize the optical contrast of the electrochromic properties, the relative concentration of P_2W_{18} and PEDOT was changed by controlling the number of P_2W_{18} in each layer and the sweeping cycles during the synthesis of the EDOT layer in each composite layer of [P_2W_{18}/PAH/P_2W_{18}/PEDOT] (see Fig. 1).

3.2 Cyclic voltammograms

Cyclic voltammetry (CV) was used to monitor the stepwise growth and elucidate the general electrochemical behavior of the films. In pH = 3 buffer solution, the CV of the P_2W_{18} solution consists of four redox peaks with formal potentials at E(I) = −0.067 V, E(II) = −0.252 V, E(III) = −0.661 V, and E(IV) = −0.942 V, where $E = (E_{pc} + E_{pa})/2$. The four couples of redox peaks correspond to four reversible (one-, one-, two-, and two-electron) reduction processes. The CV curve of the [P_2W_{18}–PAH]$_{10}$ film displays five redox peaks in the potential range −0.8

to 0.2 V with formal potentials at E(I) = −0.190 V, E(II) = −0.428 V, E(III) = −0.543 V, I(IV) = −0.616 V and E(V) = −0.690 V (Fig. S1 in ESI†). The five redox peaks are assigned to one two-electron and four one-electron redox processes. It is noted that the first two one-electron peaks in the P_2W_{18} solution merge into one two-electron peaks, and another two two-electron peaks in the P_2W_{18} solution split into four one-electron peaks in the $[P_2W_{18}–PAH]_{10}$ film. These merging and splitting phenomena of the $[P_2W_{18}–PAH]_{10}$ film is similar to that of P_2W_{18}–containing LbL films studied by Cheng and co-workers.[14] It is possible that the structure of the multilayer films, with a strong electrostatic interaction between PAH and P_2W_{18}, influences the electron transport of the redox processes.[15] Furthermore, the protonation plays an important role in the charge compensation during the redox processes. Proton diffusion is suppressed in the compact film, which causes the above merging and splitting phenomena.[16] In addition, the $[PEDOT]_{10}$ film shows a cathodic peak at −0.707 V, but the corresponding anodic peak can not be seen clearly (Fig. S1 in ESI†). The electrochemical behavior is quite different from those of PEDOT films reported previously because of different electrolytes and experimental parameters.[17]

As shown in Fig. 2a, the redox chemistry of the $[P_2W_{18}–PEDOT]_n$ (n = 2, 4, 6, 8, 10, 12,14, 16, 18, 20) films was examined by switching the potential from −0.8 to 0.2 V. The films exhibit five couples of redox waves with E(I) = −0.010 V, E(II) = −0.155 V, E(III) = −0.419 V, E(IV) = −0.530 V and E(V) = −0.667 V, which is similar to the CV curve of the $[P_2W_{18}–PAH]_{10}$ film [E, defined as $E = (E_{pc} + E_{pa})/2$]. This indicates that P_2W_{18} is effectively incorporated into the composite film. From the CVs, the electrochemical contribution of PEDOT is not identified immediately. It is inferred that the peaks of PEDOT are overlapped by those of P_2W_{18} in the potential range. In addition, Fig. 2a displays the CV curves with a function of the number of $[P_2W_{18}–PEDOT]$ layers. With the increase in the number of layers, the cathodic peak potentials shift slightly toward negative potential values and the anodic peak potentials shift toward positive potential values, which probably relates to the uncompensated resistance.[11] In the inset of Fig. 2a, the peak III currents of the $[P_2W_{18}–PEDOT]_n$ films increase linearly with the number of deposition cycles, suggesting that the growth for each deposition cycles is reproducible.

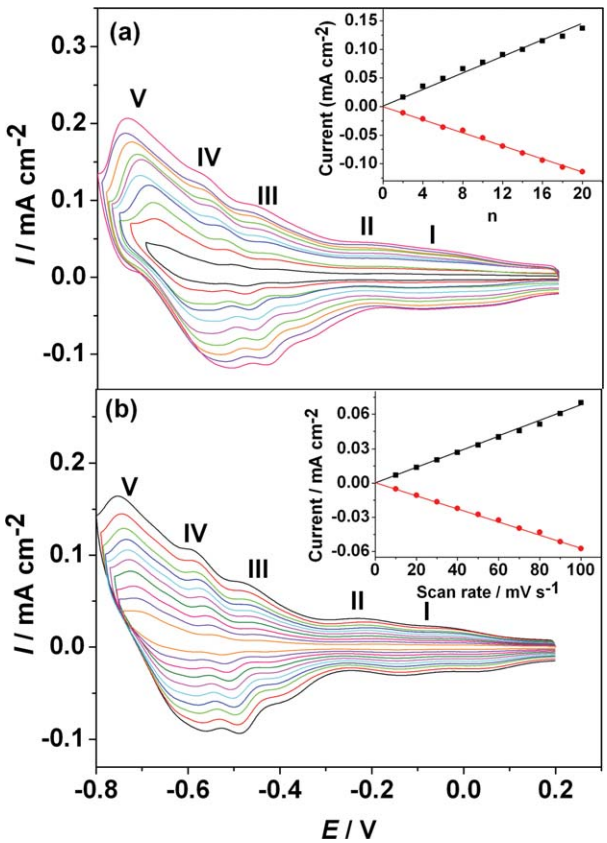

Fig. 2 (a) CV curves of $[P_2W_{18}–PEDOT]_n$ layer at a scan rate of 25 mV s^{-1} (from inner to outside: n = 2, 4, 6, 8, 10, 12,14, 16, 18, 20). The inset shows the relationship of the peak III currents as a function of n. (b) CV curves of $[P_2W_{18}–PEDOT]_4$ film at different scan rates (from inner to outside) of 10, 20, 30, 40, 50, 60, 70, 80, 90, 100 mV s^{-1}. The inset shows the relationship of the peak III currents as a function of scan rate.

Fig. 2b displays the CVs of the $[P_2W_{18}–PEDOT]_4$ film at different scan rates in the potential range −0.8 to 0.2 V. When the scan rate increases from 10 to 100 mV s^{-1}, the cathodic peak potentials shift to negative potential values while the anodic peak potentials shift to positive potential values, which is consistent with a reversible but nonideal redox process.[18] Additionally, the ΔE_p ($\Delta E_p = E_{pa} - E_{pc}$) increases with the scan rate. This phenomenon may be a result of the increasing hysteresis between the reductive and the oxidative current waves as scan rate increases. The increasing hysteresis is probably due to slow electron transfer from ITO to the electroactive materials. Taking the third pair of peaks as an example, the peak currents are linear with the scan rate, indicating that the electrochemical behavior of P_2W_{18} has the typical property of a surface confined electrochemical process.

The effect of pH values on the electrochemical behavior of the $[P_2W_{18}–PEDOT]_{20}$ film has been investigated. The plot of voltage of the last redox peaks *versus* pH displays good linearity in the pH range from 1 to 6 (Fig. S2 in ESI†). As the pH increases from 1 to 6, the peak potentials of the last redox peaks gradually shifts to more negative potential values. When the pH is increased to 6, the potential is applied to a negative limit sufficient to obtain ill-defined waves. This is primarily due to the irreversible reduction of P_2W_{18} anions in the composite film at negative potentials beyond −1.05 V.

3.3 Surface morphology

AFM and SEM can provide the detailed information concerning the surface morphology and the homogeneity of the films. Fig. 3 shows the AFM images of the precursor film and $[P_2W_{18}–PEDOT]_3$ film adsorbed on a ITO glass. Before $[P_2W_{18}–PEDOT]$ adsorption, the precursor film is uniform, with a mean roughness of 1.1 nm (Fig. 3a). After the adsorption of $[P_2W_{18}–PEDOT]_3$, the interface displays an increased mean roughness of 2.3 nm (Fig. 3b), indicating that P_2W_{18} and PEDOT were successfully fabricated into the composite film.

The surface morphologies of the PEDOT-only and the composite films were investigated by SEM. The APS precursor film is smooth (Fig. 4a), which is consistent with the previously published work.[19] However, after the deposition of

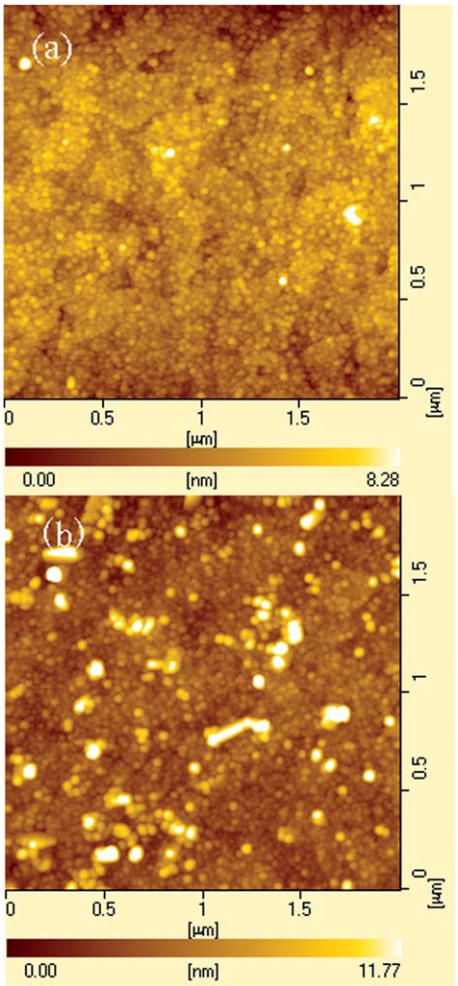

Fig. 3 AFM images of (a) the APS precursor film and (b) $[P_2W_{18}$-PEDOT$]_3$ film on a ITO glass.

$[P_2W_{18}$–PEDOT$]_{20}$, the film surface is rough. In Fig. 4c, the $[P_2W_{18}$–PEDOT$]_{20}$ film displays a regular globular microstructure intermingled with small island, which is also shown in the films containing POMs and PAH.[20] However, the PEDOT film displays a smoother surface than that of the $[P_2W_{18}$–PEDOT$]_{20}$ film (Fig. 4b). This difference could be attributed to the bi- and multilayer aggregates of the P_2W_{18} polyanions, the PAH polyelectrolyte chains, and/or PEDOT chains. Furthermore, the morphology of the PEDOT film is different to that reported in the literature.[21] It is possible that the authors used different media and experimental conditions. Fig. 4d shows the cross-section morphology of the $[P_2W_{18}$–PEDOT$]_{20}$ film prepared on ITO-coated glass. From the cross-section observations, the thickness of the multilayer film was approximately 6 μm.

3.4 Optical properties

Spectroelectrochemistry was used to evaluate the optical properties of the composite film. Fig. 5 shows the UV-vis spectra of the $[P_2W_{18}$–PEDOT$]_{20}$ film-modified ITO glass electrode under different potentials. At first, the film is light blue at an applied potential of 0 V. The absorption in the visible region at about 800 nm is attributed to the oxidized state of the PEDOT. As the potential increases from −0.5 to −1 V, an intense absorption in the range of 590–620 nm is observed owing to mixed contributions from the intervalence charge transfer band of P_2W_{18} and the π–π* transition of PEDOT. On increasing the potential to −1.5 V, the peak absorbance at 570 nm increases obviously because the π–π* transition of PEDOT gains intensity. From −1.0 to −1.5 V the coloration is primarily due to the reduction of PEDOT. It is possible that at negative potentials beyond −1.0 V, a fully reduced form of P_2W_{18} exists and no more electrochemically addressable sites are left.[22] This phenomenon is similar to that obtained from the $[P_2W_{18}$–PAH$]_{40}$ film. When the potential is switched from −1.5 to +1.0 V, both P_2W_{18} and PEDOT are oxidized, and the composite film is bleached. As shown in Fig. 5, the absorption at +1.0 V is similar to that obtained at 0 V.

Fig. 6 displays the absorption spectrum of the $[P_2W_{18}$-PEDOT$]_{20}$ film, compared with the spectra of the $[P_2W_{18}$–PAH$]_{40}$ and $[PEDOT]_{10}$ films at an applied potential of −1.0 V. Upon electrochemical reduction, the $[P_2W_{18}$–PAH$]_{40}$ film exhibits a broad adsorption band with a maximum at approximately 650 nm, which is due to the optical absorption of an

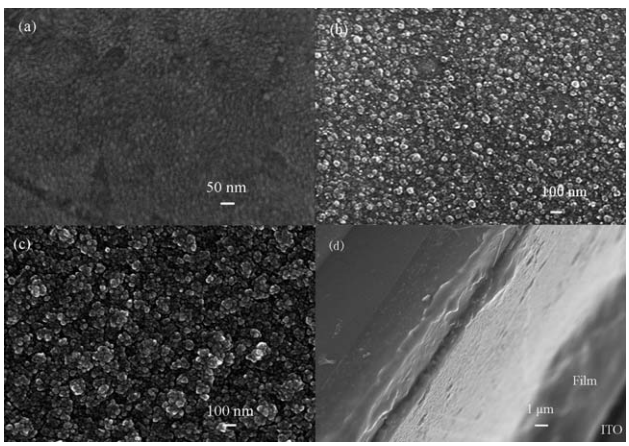

Fig. 4 SEM images of (a) the APS precursor film, (b) the PEDOT film, (c) the $[P_2W_{18}$–PEDOT$]_{20}$ film. (d) Cross-section SEM micrograph of $[P_2W_{18}$–PEDOT$]_{20}$ film on a ITO glass.

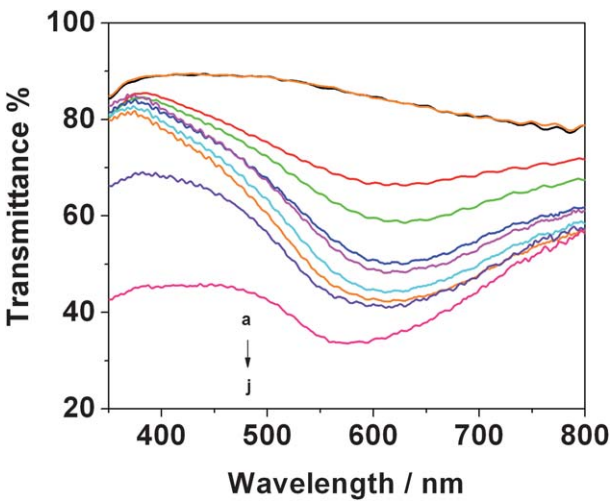

Fig. 5 UV-vis spectra of $[P_2W_{18}$–PEDOT$]_{20}$ film under different potentials (a–j: +1.0, 0, −0.5, −0.6, −0.7, −0.8, −0.9, −1.0, −1.2, −1.5 V).

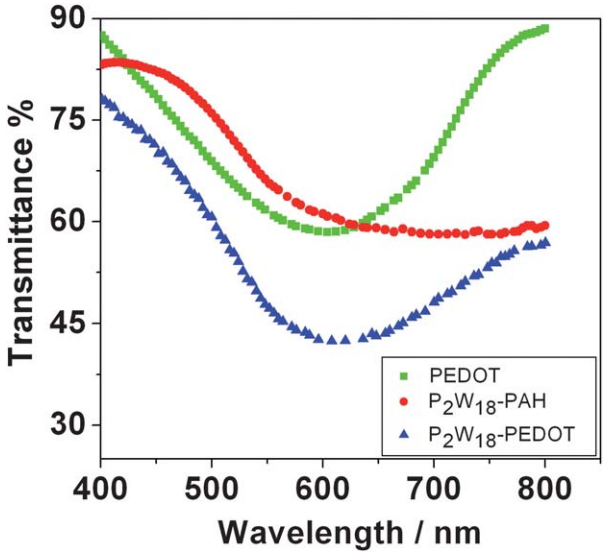

Fig. 6 Comparison of visible spectra of reduced (−1.0 V) $[P_2W_{18}$–PEDOT$]_{20}$, $[P_2W_{18}$–PAH$]_{40}$, and $[PEDOT]_{10}$ films.

intervalence charge transfer band from W^{VI} to W^{V}. In the $[PEDOT]_{10}$ film, the characteristic visible absorbance of the reduced state can be observed at 610 nm owing to the π–π* transition of PEDOT. The coloration of the $[P_2W_{18}$–PEDOT$]_{20}$ film is the result of the contribution of the two chromophores. The $[P_2W_{18}$–PEDOT$]_{20}$ film displays a broad absorption (590–620 nm), which is due to an overlap of the characteristic absorptions of P_2W_{18} and PEDOT. As shown in Fig. 6, the $[P_2W_{18}$–PEDOT$]_{20}$ film displays higher and broader absorbance than that of the single-component electrochromic films. Although the absorbance produced by the $[P_2W_{18}$–PEDOT$]_{20}$ film is a little lower than that of the addition of the individual $[P_2W_{18}$–PAH$]_{40}$ and $[PEDOT]_{10}$ films, the absorbance is significantly improved by the incorporation of P_2W_{18} into the PEDOT film.

3.5 Electrochromism

The electrochromic properties of the $[P_2W_{18}$–PEDOT$]_{20}$ film were investigated by double potential experiments as well as absorption measurements. The optical contrast (ΔT%) is probably the most important parameter in evaluating electrochromic materials. As shown in Fig. 7, the optical contrast of the $[P_2W_{18}$–PEDOT$]_{20}$ film is 54.7% under a square wave potential of −1.5 and +1.0 V, which is higher than that of $[P_2W_{18}$–PAH$]_{40}$ (42.3%) and $[PEDOT]_{10}$ (20.3%). In such case, both P_2W_{18} and PEDOT should be responsible for the electrochromic coloration, thus enhancing the optical contrast.

Consequently, the observed optical contrast is higher than that of PEDOT films electrodeposited in organic media as reported by Gaupp *et al.* (44%) and PEDOT-S/PAH films prepared by the LbL method (45%).[23,24] Additionally, it is comparable to the optical contrast of other polythiophene systems.[25] Moreover, the absorbance changes of $[P_2W_{18}$–PEDOT$]_n$ (n = 5, 10, 15 and 20) films are linear with the number of layers, as shown in Table 1. This phenomenon is indicative that all electroactive materials

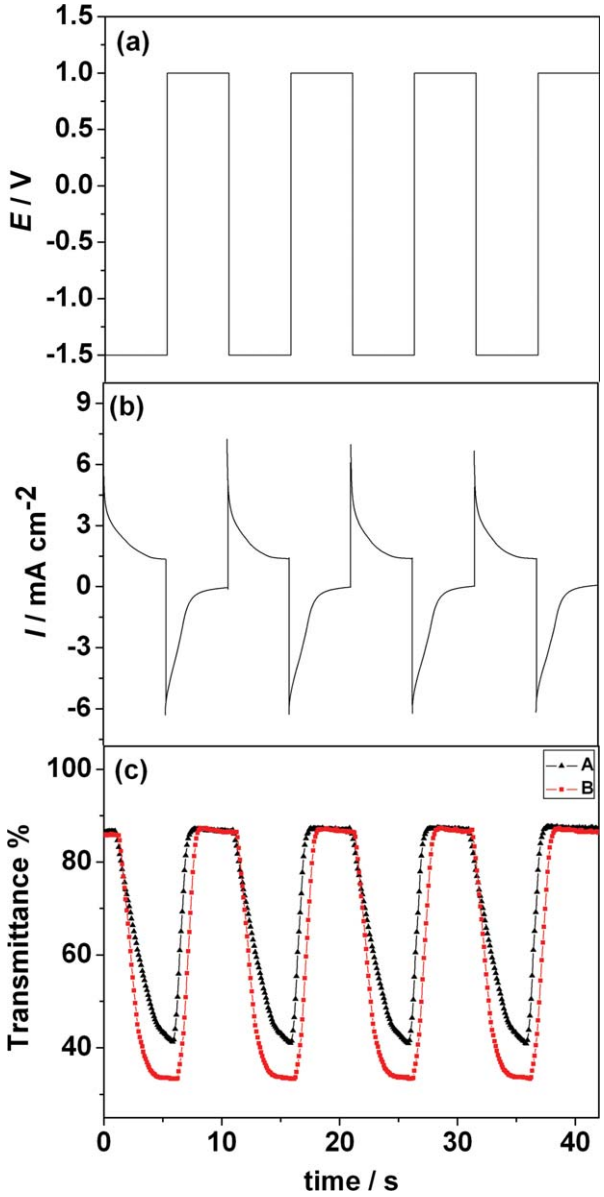

Fig. 7 (a, b) Potential and current of the $[P_2W_{18}$–PEDOT$]_{20}$ film during subsequent double potential steps at −1.5 to +1.0 V. (c) Transmittance of the $[P_2W_{18}$–PEDOT$]_{20}$ film at 600 nm under a square wave potential of (A) −1.0 and +1.0 V (B) −1.5 and +1.0 V.

Table 1 Optical contrast and switching time of $[P_2W_{18}$–PEDOT$]_n$ films during subsequent double-potential steps (−1.0 and +1.0 V) and (−1.5 and +1.0 V)

Potential	n	ΔT (%)	t_c/s	t_b/s
−1.0 and +1.0 V	5	9.4	1.34	0.28
	10	19.9	2.38	0.62
	15	31.7	3.69	0.73
	20	45.9	3.72	0.90
−1.5 and +1.0 V	5	12	0.90	0.41
	10	28.9	1.02	0.70
	15	38.8	1.70	0.88
	20	54.7	2.45	1.41

within the multilayer film are accessible during electrochemical cycling.[26]

The switching kinetics was investigated by evaluating the time defined as the requirement for 90% of the total absorbance change. In our experiments, the $[P_2W_{18}–PEDOT]_{20}$ film requires 2.4 s to color (t_c) and 1.4 s to bleach (t_b), whereas the $[P_2W_{18}–PEDOT]_5$ film takes 0.9 s for coloring and 0.4 s for bleaching. Response times of 1–2 s are the typical switching times for electrochromic polymer materials, though the times obtained here are somewhat longer than those for other films reported earlier.[27,28] In fact, the $[P_2W_{18}–PEDOT]_{20}$ film is far thicker than those with subsecond switching. The slower switching probably results from slow ion permeation and internal resistance in thick films.[26]

In addition, Table 1 reports a full tabulation of the optical switching. The observed trend in Table 1 displays three significant points. First, the electrochromic properties are strongly dependent on the number of layers. The contrast and switching times increase with the layer number. Second, the bleaching is observed to be faster than the coloration, which is in accordance with the time needed for the oxidation and reduction of the PEDOT. It parallels the very rapid access to the PEDOT structures compared with their difficult reducibility.[29] Third, the optical contrast of the $[P_2W_{18}–PEDOT]_{20}$ film at −1.5 V could increase by 16.1% compared to the optical contrast at −1.0 V.

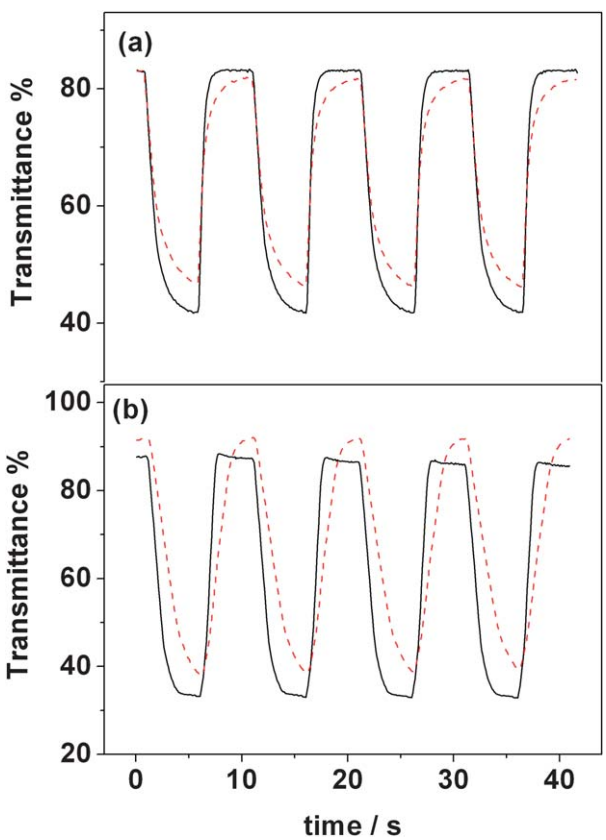

Fig. 8 The absorption changes of $[P_2W_{18}–PEDOT]_{20}$ film at 600 nm under a square wave potential of (a) −1.0 and +1.0 V (solid line: the initial cycles; dash line: after 500 cycles). (b) −1.5 and +1.0 V (solid line: the initial cycles; dash line: after 50 cycles).

Table 2 The stability of the $[P_2W_{18}–PEDOT]_{20}$ and $[PEDOT]_{10}$ films during subsequent double potential steps (−1.0 and +1.0 V) and (−1.5 and +1.0 V)

Sample	potential	stability[a] (%)	stability[b] (%)
$[P_2W_{18}–PEDOT]_{20}$	−1.0 and +1.0 V	97.9	97.3
	−1.5 and +1.0 V	92.4	36.0
$[PEDOT]_{10}$	−1.0 and +1.0 V	49.1	17.6
	−1.5 and +1.0 V	24.4	9.16

[a] Values obtained from the ratio of the absorbance of 20 cycles to the initial absorbance. [b] Values obtained from the ratio of the absorbance of 50 cycles to the initial absorbance.

This result provides the evidence that PEDOT can be further reduced, resulting in the increase of the optical contrast at negative potential beyond −1.0 V. The fully reduced form at −1.5 V may result from the presence of P_2W_{18} and the primary coloration at −1.0 V should be related to the reduction of PEDOT.[22]

The stability was evaluated by the absorbance change of the composite film. Fig. 8 displays the absorption results for the double potential experiment performed on the $[P_2W_{18}–PEDOT]_{20}$ film at 600 nm. It is found that the absorption retained 83.7% of its original value after 500 cycles and it was reduced to 76.6% of its original value after 1500 cycles under ±1 V. There is an increase in degradation when the reduction voltage varies from −1 to −1.5 V. The absorption was reduced to 36.0% of its initial value under −1.5 and +1.0 V after 50 cycles. Table 2 shows the comparison of the $[P_2W_{18}–PEDOT]_{20}$ and $[PEDOT]_{10}$ films for the same number double potential steps. The absorption of the $[PEDOT]_{10}$ film was reduced to 17.6% of its initial values after 50 cycles. The electrochemical degradation of the PEDOT film is attributed to several mechanisms. One of the important reasons is the decay of PEDOT owing to nucleophilic attack and hydrolysis of PEDOT in some aqueous electrolytes.[5] Additionally, the loss in optical contrast is possibly a result of the trapping of ions among the PEDOT chains.[30] In contrast, the $[P_2W_{18}–PEDOT]_{20}$ film presented better stability than the $[PEDOT]_{10}$ film due to the existence of an electrostatic attraction among the anionic P_2W_{18} units, the polyelectrolyte PAH, and the positively charged PEDOT.[31] Another important factor is the presence of polyelectrolyte PAH adsorbed at the interface in a condensed, coiled conformation.[18] At high ionic strength PAH can extend vertically, forming a 3-dimensional structure, which is responsible for improved stability.

4 Conclusions

A composite film composed of inorganic nanoparticles (P_2W_{18}), conductive polymer (PEDOT) and polyelectrolyte (PAH) was fabricated by the smart combination of LbL and electro-polymerization methods. The electrochromic performance of the composite film is superior to that of PEDOT-only films. The composite film displayed high optical contrast, fast response times, and long-term stability. Spectroelectrochemcial investigations demonstrated that both P_2W_{18} and PEDOT synchronously contribute to electrochromic coloration. The existence of the polyelectrolyte PAH in a condensed, coiled conformation is responsible for enhanced stability. Therefore, the

[P_2W_{18}–PEDOT] composite film becomes a promising candidate for possible applications in electrochromic devices. In addition, the smart combination of LbL and electro-polymerization methods provides a convenient means to create new composite materials based on both conductive polymers and POMs.

Acknowledgements

The authors are thankful for the financial support from the Natural Science Foundation of China (Grant No. 20731002 and 20971019). This work was also supported financially by the Fundamental Research Funds for the Central Universities (Grant No. 09SSXT122).

Notes and references

1 X. F. Lu, C. Wang and Y. Wei, *Small*, 2009, **5**, 2349–2370.
2 P. Gomez-Romero, *Adv. Mater.*, 2001, **13**, 163–174.
3 M. Fabretto, K. Zuber, C. Hall, P. Murphy and H. J. Griesser, *J. Mater. Chem.*, 2009, **19**, 7871–7878.
4 S. Bhandari, M. Deepa, A. K. Srivastava, A. G. Joshi and R. Kant, *J. Phys. Chem. B*, 2009, **113**, 9416–9428.
5 L. J. Ma, Y. X. Li, X. F. Yu, Q. B. Yang and C.-H. Noh, *Sol. Energy Mater. Sol. Cells*, 2008, **92**, 1253–1259.
6 C. L. Hill, *Chem. Rev.*, 1998, **98**, 1–2.
7 A. K. Cuentas-Gallegos, M. Lira-Cantú, N. Casañ-Pastor and P. Gómez-Romero, *Adv. Funct. Mater.*, 2005, **15**, 1125–1133.
8 A. Balamurugan and S.-M. Chen, *Electroanalysis*, 2007, **19**, 1616–1622.
9 R. G. Finke, M. W. Droege and P. J. Domaille, *Inorg. Chem.*, 1987, **26**, 3886–3896.
10 G. G. Gao, L. Xu, W. J. Wang, Z. Q. Wang, Y. F. Qiu and E. B. Wang, *Electrochim. Acta*, 2005, **50**, 1101–1106.
11 B. Wang, R. N. Vyas and S. Shaik, *Langmuir*, 2007, **23**, 11120–11126.
12 X. Du and Z. Wang, *Electrochim. Acta*, 2003, **48**, 1713–1717.
13 C. Kvarnström, H. Neugebauer, S. Blomquist, H. J. Ahonen, J. Kankare and A. Ivaska, *Electrochim. Acta*, 1999, **44**, 2739–2750.
14 L. Cheng and S. J. Dong, *J. Electroanal. Chem.*, 2000, **481**, 168–176.
15 M. H. Huang, L. H. Bi, Y. Shen, B. F. Liu and S. J. Dong, *J. Phys. Chem. B*, 2004, **108**, 9780–9786.
16 I. Moriguchi and J. H. Fendler, *Chem. Mater.*, 1998, **10**, 2205–2211.
17 C. Li and T. Imae, *Macromolecules*, 2004, **37**, 2411–2416.
18 S. Q. Liu, D. G. Kurth, B. Bredenkötter and D. Volkmer, *J. Am. Chem. Soc.*, 2002, **124**, 12279–12287.
19 G. G. Gao, L. Xu, W. J. Wang, Z. Q. Wang, Y. F. Qiu and E. B. Wang, *J. Electrochem. Soc.*, 2005, **152**, H102–H106.
20 S. P. Liu, L. Xu, G. G. Gao and B. B. Xu, *Thin Solid Films*, 2009, **517**, 4668–4672.
21 S. Bhandari, M. Deepa, A. K. Srivastava, C. Lal and R. Kant, *Macromol. Rapid Commun.*, 2008, **29**, 1959–1964.
22 M. Deepa, A. Awadhia and S. Bhandari, *Phys. Chem. Chem. Phys.*, 2009, **11**, 5674–5685.
23 C. L. Gaupp, D. M. Welsh, R. D. Rauh and J. R. Reynolds, *Chem. Mater.*, 2002, **14**, 3964–3970.
24 C. A. Cutler, M. Bouguettaya and J. R. Reynolds, *Adv. Mater.*, 2002, **14**, 684–688.
25 V. Jain, R. Sahoo, S. P. Mishra, J. Sinha, R. Montazami, H. M. Yochum, J. R. Heflin and A. Kumar, *Macromolecules*, 2009, **42**, 135–140.
26 D. M. DeLongchamp, M. Kastantin and P. T. Hammond, *Chem. Mater.*, 2003, **15**, 1575–1586.
27 A. Maier, A. R. Rabindranath and B. Tieke, *Chem. Mater.*, 2009, **21**, 3668–3676.
28 L. Motiei, M. Lahav, D. Freeman and M. E. vanderBoom, *J. Am. Chem. Soc.*, 2009, **131**, 3468–3469.
29 S. Kirchmeyer and K. Reuter, *J. Mater. Chem.*, 2005, **15**, 2077–2088.
30 J.-H. Huang, C.-Y. Hsu, C.-W. Hu, C.-W. Chu and K.-C. Ho, *ACS Appl. Mater. Interfaces*, 2010, **2**, 351–359.
31 L. Adamczyk, P. J. Kulesza, K. Miecznikowski, B. Palys, M. Chojak and D. Krawczyk, *J. Electrochem. Soc.*, 2005, **152**, E98–E103.

